Chemical Science

EDGE ARTICLE

View Article Online
View Journal | View Issue

Cite this: *Chem. Sci.*, 2014, **5**, 2340

Metal control of selectivity in acetate-assisted C–H bond activation: an experimental and computational study of heterocyclic, vinylic and phenylic C(sp^2)–H bonds at Ir and Rh†

Kevin J. T. Carr,[a] David L. Davies,*[b] Stuart A. Macgregor,*[a] Kuldip Singh[b] and Barbara Villa-Marcos[b]

Acetate-assisted C(sp^2)–H bond activation at $[MCl_2Cp^*]_2$ (M = Ir, Rh) has been studied for a series of *N*-alkyl imines, ^{i}PrN=CHR, (R = *N*-methyl-2-pyrrolyl, **H-L$_1$**; 2-furanyl, **H-L$_2$**; 2-thiophenyl, **H-L$_{3a}$**; C_2H_2Ph, **H-L$_4$**; and Ph, **H-L$_5$**) as well as phenylpyridine (**H-L$_6$**) by both experimental and computational means. Competition experiments reveal significant variation in the relative reactivity of these substrates and highlight changes in selectivity between Ir (**H-L$_4$** ≈ **H-L$_2$** < **H-L$_{3a}$** ≈ **H-L$_5$** < **H-L$_1$** ≈ **H-L$_6$**) and Rh (**H-L$_2$** ≈ **H-L$_1$** < **H-L$_{3a}$** ≈ **H-L$_4$** < **H-L$_5$** < **H-L$_6$**). Comparison of **H-L$_{3a}$** with its *N*-xylyl analogue, **H-L$_{3b}$**, gives a further case of metal-based selectivity, **H-L$_{3a}$** being more reactive at Ir, while **H-L$_{3b}$** is preferred at Rh. H/D exchange experiments suggest that the selectivity of C–H activation at Ir is determined by kinetic factors while that at Rh is determined by the product thermodynamic stability. This is confirmed by computational studies which also successfully model the order of substrate reactivity seen experimentally at each metal. To achieve the good level of agreement between experiment and computation required the inclusion of dispersion effects, use of large basis sets and an appropriate solvent correction.

Received 11th March 2014
Accepted 22nd March 2014

DOI: 10.1039/c4sc00738g

www.rsc.org/chemicalscience

Introduction

The activation of unreactive C–H bonds under mild conditions by transition metal complexes represents an atom-economical basis for the synthesis of more complex molecules. However, the vast majority of molecules of interest have not just one, but rather multiple C–H bonds that may potentially undergo activation. In order to design selective catalysts for C–H functionalization it is important to understand the kinetic and thermodynamic selectivity of the key initial C–H activation process. Whilst this can in principle be done experimentally it would be particularly advantageous if computational methods could be used to predict such selectivity. To achieve this it is important to benchmark calculated results against experimental data to ensure that an appropriate computational methodology is adopted.

Different mechanisms have been identified for the activation of C–H bonds, including radical, oxidative addition, σ-bond metathesis, 1,2-addition and electrophilic activation.[1] More recently acetate-assisted C–H activation, *via* what has been described as ambiphilic metal-ligand assistance (AMLA)[1c,2] or the related concerted metallation–deprotonation (CMD) process,[3] has become particularly important as a key step in catalytic C–H functionalization.[4] It is expected that the selectivity of C–H bond activation will depend on the mechanism involved as well as on the specific catalyst used. C–H activation *via* oxidative addition has been particularly well studied in this regard and the selectivity of this process has been linked to the strength of the M–C bond being formed.[5] In contrast, less is known about the selectivity of C–H activation by the AMLA/CMD mechanism. Fagnou and Gorelsky have used density functional theory (DFT) calculations to assess substituent effects on the barrier to the C–H activation step for a range of (hetero) aromatics reacting at $Pd(OAc)_2$. For 2-substituted thiophenes a reasonable correlation between barrier height and reactivity towards direct arylation was seen, with electron-donating substituents promoting the reaction, implying kinetic control in that case.[3b,6] The choice of anion, acetate or carbonate, can also affect the selectivity of C–H activation.[7]

Thiophenes and other heterocycles are important components of many pharmaceuticals and agrochemicals, and although a few examples of stoichiometric[2a,8] and catalytic[9] C–H functionalisation of such species are present in the literature,

[a]*Institute of Chemical Sciences, Heriot-Watt University, Edinburgh EH14 4AS, UK. E-mail: S.A.Macgregor@hw.ac.uk*

[b]*Department of Chemistry, University of Leicester, Leicester LE1 7RH, UK. E-mail: dld3@leicester.ac.uk*

† Electronic supplementary information (ESI) available. CCDC 980293–980300. For ESI and crystallographic data in CIF or other electronic format see DOI: 10.1039/c4sc00738g

few detailed mechanistic studies have been reported. Herein, we describe such a study that combines both experiment and computation to study the mechanism and selectivity of acetate-assisted C–H activation of a range of imines with heterocyclic, vinyl and phenyl substituents at $[MCl_2Cp^*]_2$ complexes (M = Ir, Rh). Competition experiments reveal significant changes in the relative reactivity of a series of closely related C(sp^2)–H bonds and highlight how the selectivity of C–H activation may be controlled by changing between the Ir and Rh metal centres. The DFT calculations provide insight into the basis of this selectivity and direct comparison with experiment shows that the observed selectivities can be successfully reproduced by the calculations once dispersion, solvation and basis set effects are taken into account.

Results and discussion

Experimental studies

The substrates used in this study (Fig. 1) fall into three categories: heterocyclic (**H-L$_{1-3}$**), vinyl (**H-L$_4$**) and phenyl (**H-L$_{5-6}$**) derivatives. *N*-Alkyl imines were chosen since they are readily available and can act as efficient directing groups at Ir and Rh, while **H-L$_6$** provided an alternative *N*-directing group. An *N*-aryl imine (**H-L$_{3b}$**) was also included as we have previously shown the *N*-imine substituent can affect the outcome of the cyclometallation reaction.[10]

The reactivity of substrates **H-L$_{1-6}$** with $[MCl_2Cp^*]_2$ (M = Ir, Rh) was investigated as outlined in Scheme 1. With $[IrCl_2Cp^*]_2$ C–H activation of **H-L$_{1-6}$** proceeded smoothly in both dichloromethane and methanol to give the corresponding cyclometallated products (**Ir-L$_{1-6}$**) in good yields. In contrast, the synthesis and isolation of the cyclometallated Rh(III) analogues proved more challenging.[11] Thus, while full conversion was obtained after 6 hours with **H-L$_{3a}$** and $[IrCl_2Cp^*]_2$ in dichloromethane, only 34% conversion was obtained for the analogous reaction with $[RhCl_2Cp^*]_2$ in 17 h. As a result fewer cyclometallated complexes of Rh proved amenable to isolation (see ESI†).

The structures of several of the cyclometallated products were obtained by X-ray diffraction and those of **Ir-L$_1$**, **Ir-L$_{3a}$**, **Ir-L$_4$** and **Rh-L$_{3a}$** are shown in Fig. 2. Full details of these structures, along with those of **Ir-L$_{3b}$**, **Ir-L$_5$**, **Rh-L$_{3b}$** and **Rh-L$_4$** can be found in the ESI.† It is notable that there are no significant differences in the M(1)–C(3) bond lengths, despite the range of cyclometallated substrates involved. In particular the structural data for **Ir-L$_{3a}$** and **Rh-L$_{3a}$** do not provide any obvious clues to the relative stability and reactivity of these complexes.

The reversibility of C–H activation was assessed by a series of deuteration experiments by treating **H-L$_{1-6}$** with catalytic amounts of $[MCl_2Cp^*]_2$ (M = Ir, Rh) and NaOAc in d^4-MeOD (see Table S1 in ESI†). For Ir, only **H-L$_1$** showed any evidence for H/D exchange (20% deuteration after 10 days) even in the presence of pivalic acid. In contrast, for Rh all the ligands except **H-L$_4$** and **H-L$_6$** exhibited H/D exchange at the C(sp^2)–H bond exposed to cyclometallation.[12] Deuterium incorporation into **H-L$_1$** was particularly fast, with full H/D exchange being achieved after 3 hours; for the other substrates 50% incorporation generally required 4–10 days. For **H-L$_4$** and **H-L$_6$** addition of pivalic acid was necessary to observe deuteration. These results indicate that the C–H activation is generally irreversible at Ir under the conditions employed, but reversible at Rh, albeit with higher barriers to the reverse reaction with **H-L$_4$** and **H-L$_6$**. This in turn suggests that Ir should show kinetic selectivity while with Rh

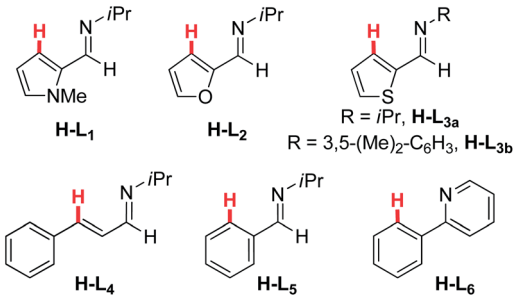

Fig. 1 Substrates used for the C–H activation studies.

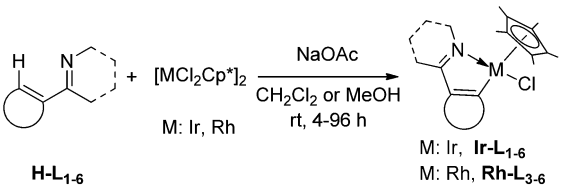

Scheme 1 Reaction conditions for cyclometallation at $[MCl_2Cp^*]_2$ (M = Ir, Rh).

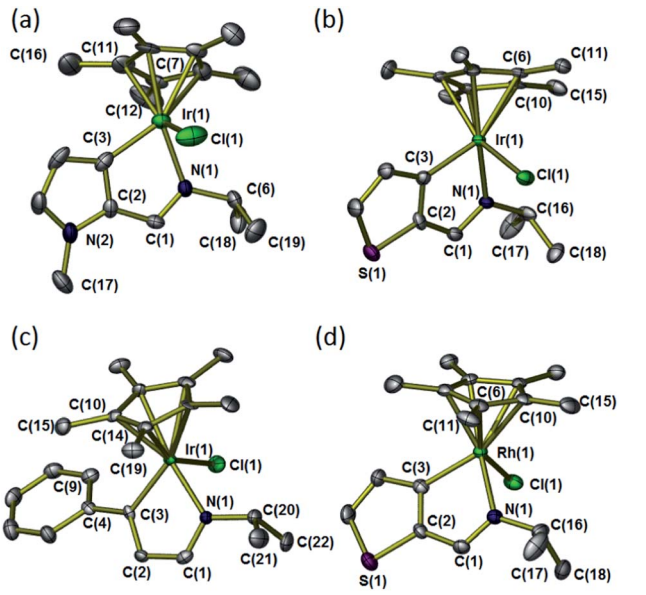

Fig. 2 Molecular structures and atom numbering schemes for (a) **Ir-L$_1$**, (b) **Ir-L$_{3a}$**, (c) **Ir-L$_4$** and (d) **Rh-L$_{3a}$**. Thermal ellipsoids are drawn at 50% probability level, and hydrogen atoms are omitted for clarity. Selected bond lengths [Å], **Ir-L$_1$**: Ir–C3: 2.049(9); Ir–N1: 2.107(6); **Ir-L$_{3a}$**: Ir–C3: 2.027(5); Ir–N1: 2.102(4); **Ir-L$_4$**: Ir–C3: 2.031(5); Ir–N1: 2.084(5). **Rh-L$_{3a}$**: Rh–C3: 2.018(4); Rh–N1: 2.114(3).

the products are forming under thermodynamic control. This is also consistent with the DFT calculations (see below).

The relative reactivities of the different heterocyclic, vinyl and aryl C(sp^2)–H bonds in **H-L$_{1-6}$** were further assessed through a series of competition reactions in which a 1 : 1 molar ratio of two different substrates was treated with 10 mol% of $[MCl_2Cp^*]_2$ (M = Ir, Rh) in the presence of 40 mol% NaOAc.

The ratios of the cyclometallated products were determined by ^{1}H NMR spectroscopy (see Tables S2 and S3 in the ESI† for full details). In a representative experiment, the reaction of **H-L$_2$** and **H-L$_{3a}$** afforded cyclometallated products **Ir-L$_2$** and **Ir-L$_{3a}$** in a ratio of 1 : 11 (Scheme 2).[13]

The overall reactivity trends are shown in Fig. 3. For both Ir and Rh the phenylpyridine derivative **H-L$_6$** undergoes C–H activation most readily. For Ir (Fig. 3(a)) the pyrrole imine **H-L$_1$** is the next most favoured substrate, followed by phenylimine **H-L$_5$** and thiophene imine **H-L$_{3a}$**. The furan (**H-L$_2$**) and vinyl substrates (**H-L$_4$**) are clearly the least reactive at Ir. For Rh a different order is seen, with pyrrole **H-L$_1$** now among the least reactive substrates along with the furan derivative (Fig. 3(b)). A 20-fold increase in selectivity is seen in moving to thiophene **H-L$_{3a}$**, and vinyl **H-L$_4$** followed by further significant increases in selectivity to phenylimine **H-L$_5$** and finally phenylpyridine **H-L$_6$**. In general, the Rh system suggests a greater potential for selectivity as it discriminates more effectively between the different substrates. It is worth noting that the initial results obtained at Rh with vinyl substrate **H-L$_4$** suggested a far lower reactivity than shown in Fig. 3(b). In this case DFT calculations (see below) suggested that this was out of place based on the computed thermodynamic stability of the product. Hence to ensure full equilibration, pivalic acid was added to the competition experiments for Rh.

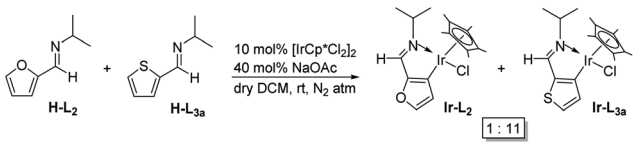

Scheme 2 Competition experiment between heterocyclic imines H-L$_2$ and H-L$_{3a}$.

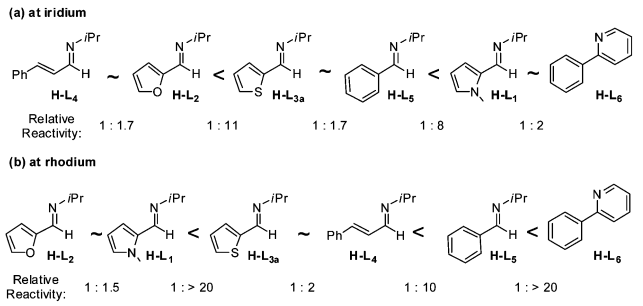

Fig. 3 Relative reactivity of ligands H-L$_{1-6}$ in competitive C–H activation reactions at (a) $[IrCl_2Cp^*]_2$ in dichloromethane and (b) $[RhCl_2Cp^*]_2$ in MeOH; figures for Rh in the presence of pivalic acid except H-L$_1$/H-L$_2$.

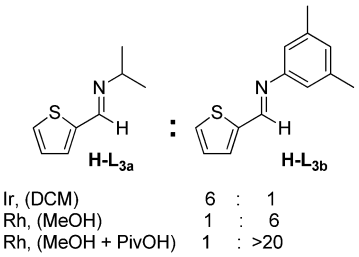

Fig. 4 Relative reactivity of ligands H-L$_{3a}$ and H-L$_{3b}$ towards C–H activation at $[MCl_2Cp^*]_2$ (M = Ir, Rh) species.

We have previously shown[10] that varying the *N*-imine substituent can affect the outcome of the cyclometallation reaction. A competition experiment was therefore run comparing the *N*-alkyl imine thiophene derivative **H-L$_{3a}$** to an *N*-aryl analogue **H-L$_{3b}$** which features an *N*-xylyl substituent (Fig. 4). For Ir the *N*-alkyl imine is favoured by a factor of 6, whereas for Rh the selectivity is reversed with a 6 : 1 ratio in favour of the *N*-aryl imine. Rerunning the Rh competition experiment in the presence of pivalic acid increased this ratio to >20 : 1.

Computational studies

To understand the different reactivity patterns observed at the Ir and Rh $[MCl_2Cp^*]_2$ species we have modelled the C–H activation reaction profiles for substrates **H-L$_{1-6}$** with DFT calculations.[14] These are based on the mechanism outlined in Fig. 5 which is illustrated for the case of substrate **H-L$_{3a}$**. Initial opening of the $[MCl_2Cp^*]_2$ dimer (denoted **I$_M$** in the computational study) with acetate may produce either [MCl(OAc)Cp*], **II$_M$**, and/or [M(OAc)$_2$Cp*], **III$_M$**. Substitution of Cl^- (in **II$_M$**) or OAc^- (in **III$_M$**) by **H-L$_{3a}$** then yields **IV$_{M\text{-}3a}$** from which C–H activation proceeds to give cyclometallated **VI$_{M\text{-}3a}$**. Depending on the system C–H activation may be a one- or two-step process, where the latter involves an agostic/H-bonded intermediate such as **V$_{M\text{-}3a}$**. HOAc/Cl^- substitution in **VI$_{M\text{-}3a}$** gives the final observed products **VII$_{M\text{-}3a}$**, equivalent to **M-L$_{3a}$** defined in the experimental study.

In order to assess the effects of basis set and functional choice we focused initially on the dimer opening process for $[RhCl_2Cp^*]_2$ and the overall free energy change for forming the cyclometallated product **VII$_{Rh\text{-}3a}$** (see Table 1). Experimentally the reaction of $[RhCl_2Cp^*]_2$ with 3 equiv. of NaOAc in MeOH leads to an equilibrium mixture of **I$_{Rh}$**, **II$_{Rh}$** and **III$_{Rh}$** indicating that these species should be close in energy.[10,11] Moreover, our observations indicate that the formation of **VII$_{Rh\text{-}3a}$** is thermodynamically favoured. Using the BP86 functional and the smaller basis set employed for optimisation (BS1) we found the relative stability in MeOH of both **II$_{Rh}$** and (in particular) **III$_{Rh}$** to be grossly overestimated, suggesting that **III$_{Rh}$** would be the only species observed in solution and ruling out any possibility of cyclometallation (Entry 1, Table 1). The situation improves somewhat when a larger basis set with diffuse functions on the ligand atoms is used (BS2, Entry 2). **II$_{Rh}$** and **III$_{Rh}$** are now closer in free energy, but both are significantly more stable than **I$_{Rh}$**

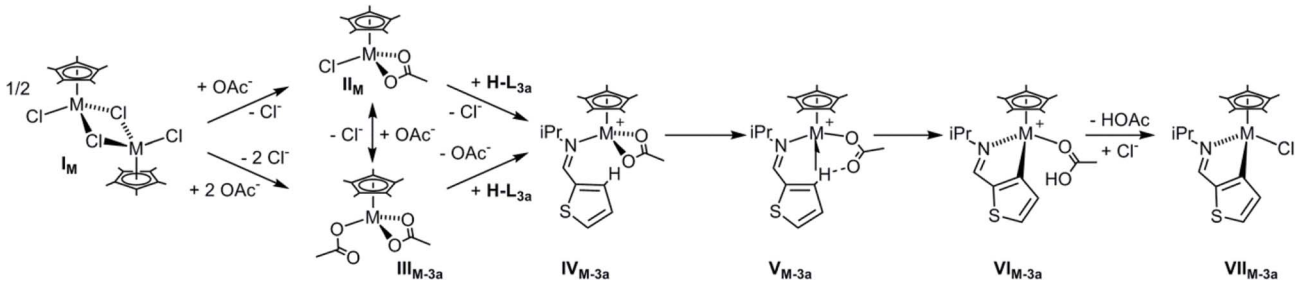

Fig. 5 Mechanism and labelling scheme employed in the computational study, illustrated for the reaction of **H-L$_{3a}$** at $[MCl_2Cp^*]_2$ (I_M, M = Ir, Rh).

Table 1 Basis set and functional testing on the free energies (kcal mol^{-1}) of formation of II_{Rh}, III_{Rh} and VII_{Rh} from I_{Rh} and **H-L$_{3a}$**. All energies include a correction for MeOH solvent

Entry	Functional/basis set	$\mathbf{II_{Rh}}$	$\mathbf{III_{Rh}}$	$\mathbf{VII_{Rh}}$	ΔG^a
1	BP86/BS1[b]	−25.4	−46.5	−27.1	+19.4
2	BP86/BS2[c]	−8.6	−5.1	−1.3	+7.3
3	BP86-D3/BS2	−1.3	−0.4	−5.3	−4.0
4	B3PW91-D3/BS2	−1.5	−0.7	−4.2	−2.7
5	PBE-D3/BS2	−3.3	+1.3	−3.5	−0.2
6	PBE0-D3/BS2	−2.9	−1.9	−3.4	−0.5
7	BLYP-D3/BS2	−2.8	−1.9	−2.0	+0.8
8	B3LYP-D3/BS2	−3.2	−3.2	−1.5	+1.7
9	M06/BS2	−2.1	−0.6	+0.4	+2.5
10	M06L/BS2	−7.2	−10.6	+2.1	+12.7
11	ωB97XD	−6.7	−7.3	−5.2	+2.1
12	B97D/BS2	−4.8	−5.2	−7.3	−2.1

[a] ΔG: difference between the most stable precursor and $\mathbf{VII_{Rh}}$. [b] BS1: Rh, S: SDD (polarisation on S), C, H, N, O: 6-31g**. [c] BS2: Rh: cc-pVTZ-PP; S, C, H, N, O: 6-311++g**.

and, in particular, the formation of $\mathbf{VII_{Rh}}$ from $\mathbf{II_{Rh}}$ remains strongly endergonic by 7.3 kcal mol^{-1}. Test calculations indicate that no significant additional improvement in the computed energetics is obtained by expanding the basis set further (see Table S5, ESI†).

Ultimately the key to obtaining reasonable energetics for these systems is the inclusion of a dispersion correction using Grimme's D3 parameter set.[15] Thus with BP86-D3/BS2 (Entry 3) $\mathbf{I_{Rh}}$, $\mathbf{II_{Rh}}$ and $\mathbf{III_{Rh}}$ all lie within 1.3 kcal mol^{-1} of each other and cyclometallation to form $\mathbf{VII_{Rh\text{-}3a}}$ is exergonic by 4.0 kcal mol^{-1}. The D3 correction also provided improved energetics for a range of other functionals (Entries 4–6), which otherwise gave highly endergonic product formation (see Table S6, ESI†). With BLYP-D3 and B3LYP-D3 $\mathbf{VII_{Rh}}$ remains slightly endergonic even with the dispersion correction (Entries 7 and 8). Interestingly the inclusion of dispersion effects within the functional was less successful, with M06 M06L and ωB97XD (Entries 9–11) all underestimating the stability of $\mathbf{VII_{Rh\text{-}3a}}$. With B97D (Entry 12) the formation of $\mathbf{VII_{Rh}}$ is computed to be thermodynamically favoured. Clearly it is important to account for the additional dispersive stabilisation associated with the close proximity of the substrate and {RhClCp*} fragments present in $\mathbf{VII_{Rh\text{-}3a}}$. However the energetics are sensitive to the way in which this is included in the computational protocol, and use of a separate empirical correction appears to perform best in this case. In the following we shall report energetics based on the BP86-D3/BS2 protocol.[16]

Full computed profiles for **H-L$_{3a}$** reacting at both $[MCl_2Cp^*]_2$ species are shown in Fig. 6 for M = Ir (blue) and Rh (red), where free energies are reported in both MeOH (plain text) and dichloromethane (italics). The discussion will focus on the results in MeOH, before considering the effects of changing solvent. After dimer opening Cl^- substitution in $\mathbf{II_M}$ (or OAc^- substitution in $\mathbf{III_M}$) with **H-L$_{3a}$** produces [M(OAc)(**H-L$_{3a}$**)Cp*], $\mathbf{IV_{M\text{-}3a}}$, the immediate precursor to C–H activation. Although endergonic, these processes are readily accessible in MeOH ($\Delta G \leq +2.6$ kcal mol^{-1}) For $\mathbf{IV_{Rh\text{-}3a}}$ C–H activation is a two-step process, κ^2–κ^1-acetate displacement giving $\mathbf{V_{Rh\text{-}3a}}$ from which intramolecular proton transfer leads to cyclometallated $\mathbf{VI_{Rh\text{-}3a}}$ at +5.7 kcal mol^{-1}. For Ir the κ^2–κ^1 displacement transition state ($G = +8.2$ kcal mol^{-1}) leads directly to C–H activated $\mathbf{VI_{Ir\text{-}3a}}$ ($G = -1.1$ kcal mol^{-1}). HOAc/Cl^- substitution then gives the final products, $\mathbf{VII_{M\text{-}3a}}$, and this exergonic step ($\Delta G = -13.1$ and -11.0 kcal mol^{-1} for M = Ir and Rh respectively) ultimately makes both these reactions thermodynamically favourable. Overall the reactions of **H-L$_{3a}$** at Ir and Rh in MeOH proceed with very similar overall barriers ($\Delta G^{\ddagger} = 10.5$ and 11.8 kcal mol^{-1} respectively). In contrast, C–H activation at Ir is significantly more exergonic ($\Delta G = -11.9$ kcal mol^{-1} *cf.* −4.0 kcal mol^{-1} for Rh). Note that these energetics are quoted relative to the most stable precursor complex in each case, *i.e.* $\mathbf{II_{Rh}}$ (at −1.3 kcal mol^{-1}) and $\mathbf{II_{Ir}}$ (at −2.3 kcal mol^{-1}). The computed results are therefore consistent with C–H activation of **H-L$_{3a}$** being irreversible at Ir, but reversible at Rh, the reverse barriers from $\mathbf{VII_{M\text{-}3a}}$ being 22.4 kcal mol^{-1} for Ir but only 15.8 kcal mol^{-1} for Rh. The calculations therefore confirm that C–H activation is under kinetic control at Ir but under thermodynamic control at Rh.

Experimentally we found it more convenient to conduct the competition experiments for Ir in dichloromethane and so we have recomputed the free energies correcting for this solvent (results in italics in Fig. 6). The major solvent-dependency is seen in the overall barriers to C–H activation and this reflects the fact that the activation energies include a contribution from the formation of $\mathbf{IV_{M\text{-}3a}}$ *via* substitution of Cl^- in $\mathbf{II_M}$ (or OAc^- in $\mathbf{III_M}$) by neutral **H-L$_{3a}$**. Such steps are less accessible in dichloromethane (*e.g.* $\mathbf{II_{Ir}} \rightarrow \mathbf{IV_{Ir\text{-}3a}}$, $\Delta G = +7.5$ kcal mol^{-1}) than

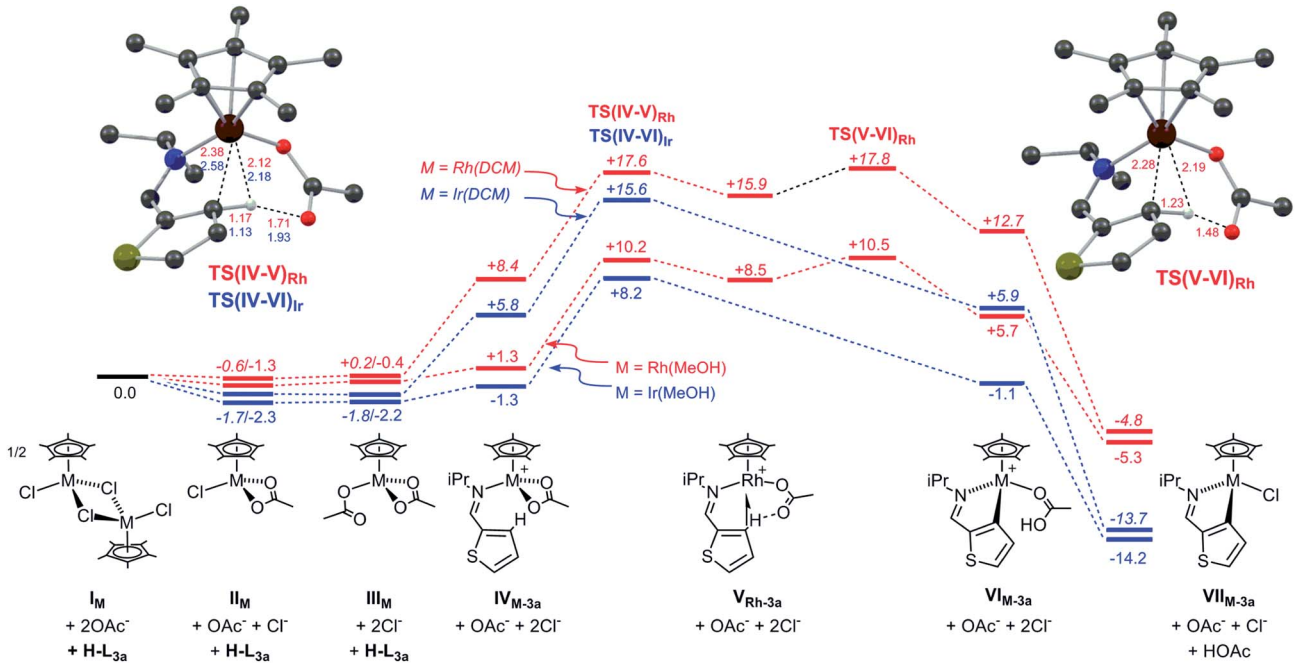

Fig. 6 Computed reaction profiles for C–H activation of **H-L$_{3a}$** at $[MCl_2Cp^*]_2$ for M = Ir (in blue) and M = Rh (in red) with energies (kcal mol^{-1}) computed in both MeOH (plain text) and dichloromethane (in italics). Computed transition state structures associated with the C–H activation steps are shown with key distances in Å and non-participating H atoms omitted for clarity.

MeOH (ΔG = +1.0 kcal mol^{-1}). The corollary is that HOAc/Cl$^-$ substitution (**VI$_{Ir\text{-}3a}$** → **VII$_{Ir\text{-}3a}$**) is much more favourable in dichloromethane (ΔG = −19.6 kcal mol^{-1}) than in MeOH (ΔG = −13.1 kcal mol^{-1}). Thus while the computed barriers are solvent dependent, the overall thermodynamics are not significantly so, indicating that the Ir system will remain under kinetic control and Rh under thermodynamic control, irrespective of the solvent used. For Rh the higher barriers computed in dichloromethane are also consistent with the slower reactions seen experimentally as the system takes longer to reach equilibrium.

Similar reaction profiles were also characterized for the other substrates under consideration and the key computed $\Delta G^{\ddagger}$ and ΔG values are shown in Table 2, where the solvents used in the experimental competition experiments are now employed. Details of the full reaction profiles are provided in the ESI.† For Ir $\Delta G^{\ddagger}$ values give the substrate reactivity trend as **H-L$_2$** < **H-L$_{3a}$** < **H-L$_5$** ≈ **H-L$_4$** < **H-L$_6$** ≈ **H-L$_1$** and this mimics the experimental pattern well, with the exception of **H-L$_4$** which has a lower than expected barrier. We comment on this issue below. For Rh the trend in substrate reactivity based on ΔG is **H-L$_1$** ≈ **H-L$_2$** < **H-L$_{3a}$** < **H-L$_5$** < **H-L$_6$** ≈ **H-L$_4$**, again in good agreement with experiment, although once more **H-L$_4$** stands out in being more favoured compared to the experimental order. We also compared the *N*-alkyl substrate **H-L$_{3a}$** and its *N*-aryl analogue **H-L$_{3b}$** and showed that the latter gives greater product stability (*i.e.* more favoured) at Rh, but a slightly increased barrier (*i.e.* less favoured) at Ir, reproducing the subtleties of the metal-controlled selectivity seen experimentally in the competition reaction between these two species (see Fig. 4). The same trends are found when the Ir system is computed in MeOH and Rh in dichloromethane, *i.e.* the observed selectivity reflects the choice of metal centre rather than the solvent employed.

Table 2 Computed energetics (kcal mol^{-1}) for C–H activation at $[MCl_2Cp^*]_2$ for M = Ir (in dichloromethane) and M = Rh (in MeOH)[a]

	M = Ir (CH_2Cl_2)		M = Rh (MeOH)	
Substrate	$\Delta G^{\ddagger}$	ΔG	$\Delta G^{\ddagger}$	ΔG
H-L$_1$	14.1	−8.6	8.1	−1.2
H-L$_2$	19.1	−9.4	14.4	−1.6
H-L$_{3a}$	17.4	−11.9	11.8	−4.0
H-L$_{3b}$	18.4	−14.4	13.5	−6.8
H-L$_4$	15.1	−16.0	13.7	−7.8
H-L$_4$'[b]	19.5	−13.1	13.0	−4.6
H-L$_5$	15.6	−13.7	11.3	−6.4
H-L$_6$	14.5	−14.5	9.1	−7.7

[a] Values are quoted relative to **II$_{Rh}$** at −1.3 kcal mol^{-1} and **III$_{Ir}$** at −1.8 kcal mol^{-1}. [b] Data computed with a C_2H_3 substituent.

Overall the calculations provide a very good description of the observed reactivity trends. Experimentally, **H-L$_1$** showed the greatest propensity toward H/D exchange in d^4-methanol and indeed was the only substrate to show this at Ir. Consistent with this, the calculations indicate that for both metals this substrate has the lowest barrier for the reverse reprotonation reaction from **VII$_{M\text{-}1a}$**.[17] The different thermodynamic and kinetic factors at play also account for the fact that **H-L$_1$** can be both one of the most reactive substrates at Ir while at the same time is the least favoured substrate at Rh. This raises the possibility of controlling the selectivity of C–H activation through an appropriate choice of metal centre. A significant contribution to this arises

from the more favourable energy change for the C–H activation step, *i.e.* for $\mathbf{IV_{M\text{-}3a}} \rightarrow \mathbf{VI_{M\text{-}3a}}$ $\Delta G = +0.1$ kcal mol^{-1} for Ir (in dichloromethane), compared to +4.4 kcal mol^{-1} for Rh (in MeOH, see Fig. 6). This probably reflects the stronger M–hydrocarbyl bond that is formed with the 3rd row metal, a feature that also promotes the thermodynamics of oxidative addition at low-valent complexes at Ir over Rh.

One exception to the good computed trends in reactivity is the general over-estimation of the reactivity of substrate **H-L$_4$**. We believe this reflects the different size of the vinyl C_2H_2Ph substituent in this species compared to **H-L$_{1\text{–}3a}$** and **H-L$_5$** where the substituents are more closely related geometrically. As a result the dispersion stabilizations that arise from the additional intramolecular interactions introduced upon substrate binding to the metal fragment are somewhat larger for **H-L$_4$** than for the other substrates, resulting in an exaggerated stability of all stationary points involving **H-L$_4$**. Thus $\Delta G^{\ddagger}$ is underestimated at Ir and ΔG is overestimated (more negative) with Rh for this substrate. To test this we recomputed this system with a smaller C_2H_3 substituent (**H-L$_{4'}$**, Table 2) and indeed computed both an increase in $\Delta G^{\ddagger}$ at Ir and a reduction in ΔG at Rh.

Conclusion

Experimental and computational studies on the relative reactivity towards acetate-assisted C(sp^2)–H activation in a series of imines featuring heterocyclic, vinyl and phenyl substituents at $[MCl_2Cp^*]_2$ (M = Ir, Rh) have revealed a strongly metal-dependent behaviour. For a given substrate lower yields were generally obtained with Rh compared to the equivalent reactions at Ir. This is linked to the reversibility of C–H activation at Rh, which is also apparent in deuteration experiments in d^4-methanol which demonstrate accessible H/D exchange for Rh, but showed this to be inaccessible (or at best very slow) with Ir. The reversibility of C–H activation with Rh has also been observed in several catalytic reactions, and in these cases it is presumably the subsequent substitution and/or insertion steps that make the overall cycle thermodynamically favourable.[18] Our results show that with some substrate/metal combinations (*e.g.* vinyl imine **H-L$_4$** and *N*-aryl imine **H-L$_{3b}$** with Rh) the equilibrium may not be fully established at room temperature and this may affect the selectivity. In these cases addition of pivalic acid has a considerable effect on the outcome, implying that the use of this additive may also affect the selectivity in catalytic reactions where activation at different C–H groups is possible.

DFT calculations using a BP86-D3 protocol successfully model and provide insight into the different reactivity patterns seen with Ir and Rh. In particular, they confirm the experimental results indicating kinetic control of C–H activation at Ir and thermodynamic control at Rh. The use of a dispersion correction, large basis sets and appropriate solvent corrections were all important if the overall behaviour of these systems is to be correctly reproduced. This system therefore adds to previous examples where a treatment of dispersion effects is vital to model a ligand dissociation or association step correctly.[18,19] The relative substrate reactivities are also well reproduced, although our work does highlight remaining challenges, in particular when considering substitution reactions of substrates of different size. Nevertheless this combined experimental and computational study is anticipated to provide a platform for the rational design of selective catalysts for the C–H activation of more complex molecules.

Experimental

Details of the experimental procedures and full characterization of the isolated complexes are included in the ESI† as is the X-ray crystal data for all the structures. Coordinates have been deposited with the Cambridge crystallographic database (CCDC 980293–980300). Full details of the calculations, functional testing and Cartesian coordinates are in the ESI.†

Acknowledgements

We thank the EPSRC for funding through awards EP/J002712/1 (SAM, KJTC) and EP/J002917/1 (BVM, DLD).

Notes and references

1 (*a*) M. Albrecht, *Chem. Rev.*, 2010, **110**, 576–623; (*b*) D. Balcells, E. Clot and O. Eisenstein, *Chem. Rev.*, 2010, **110**, 749–823; (*c*) Y. Boutadla, D. L. Davies, S. A. Macgregor and A. I. Poblador-Bahamonde, *Dalton Trans.*, 2009, 5820–5831; (*d*) J. R. Webb, S. A. Burgess, T. R. Cundari and T. B. Gunnoe, *Dalton Trans.*, 2013, 16646–16665.

2 (*a*) D. L. Davies, S. M. A. Donald, O. Al-Duaij, J. Fawcett, C. Little and S. A. Macgregor, *Organometallics*, 2006, **25**, 5976–5978; (*b*) D. L. Davies, S. M. A. Donald, O. Al-Duaij, S. A. Macgregor and M. Polleth, *J. Am. Chem. Soc.*, 2006, **128**, 4210–4211; (*c*) D. L. Davies, S. M. A. Donald and S. A. Macgregor, *J. Am. Chem. Soc.*, 2005, **127**, 13754–13755.

3 (*a*) S. I. Gorelsky, D. Lapointe and K. Fagnou, *J. Am. Chem. Soc.*, 2008, **130**, 10848–10849; (*b*) D. Lapointe and K. Fagnou, *Chem. Lett.*, 2010, **39**, 1119–1126.

4 (*a*) L. Ackermann, *Chem. Rev.*, 2011, **111**, 1315–1345; (*b*) G. Y. Song, F. Wang and X. W. Li, *Chem. Soc. Rev.*, 2012, **41**, 3651–3678; (*c*) J. Wencel-Delord, T. Droge, F. Liu and F. Glorius, *Chem. Soc. Rev.*, 2011, **40**, 4740–4761.

5 (*a*) E. Clot, C. Megret, O. Eisenstein and R. N. Perutz, *J. Am. Chem. Soc.*, 2009, **131**, 7817–7827; (*b*) Y. Z. Jiao, J. Morris, W. W. Brennessel and W. D. Jones, *J. Am. Chem. Soc.*, 2013, **135**, 16198–16212.

6 (*a*) S. I. Gorelsky, D. Lapointe and K. Fagnou, *J. Org. Chem.*, 2012, **77**, 658–668; (*b*) B. Liegault, I. Petrov, S. I. Gorelsky and K. Fagnou, *J. Org. Chem.*, 2010, **75**, 1047–1060.

7 I. A. Sanhueza, A. M. Wagner, M. S. Sanford and F. Schoenebeck, *Chem. Sci.*, 2013, **4**, 2767–2775.

8 (*a*) L. Cuesta, T. Soler and E. P. Urriolabeitia, *Chem.–Eur. J.*, 2012, **18**, 15178–15189; (*b*) S. Tollari, F. Demartin, S. Cenini, G. Palmisano and P. Raimondi, *J. Organomet. Chem.*, 1997, **527**, 93–102.

9 (*a*) T. K. Hyster and T. Rovis, *J. Am. Chem. Soc.*, 2010, **132**, 10565–10569; (*b*) A. Maehara, H. Tsurugi, T. Satoh and

M. Miura, *Org. Lett.*, 2008, **10**, 1159–1162; (*c*) S. Mochida, N. Umeda, K. Hirano, T. Satoh and M. Miura, *Chem. Lett.*, 2010, **39**, 744–746; (*d*) D. Takeda, M. Yamashita, K. Hirano, T. Satoh and M. Miura, *Chem. Lett.*, 2011, **40**, 1015–1017; (*e*) T. Ueyama, S. Mochida, T. Fukutani, K. Hirano, T. Satoh and M. Miura, *Org. Lett.*, 2011, **13**, 706–708; (*f*) P. Villuendas and E. P. Urriolabeitia, *J. Org. Chem.*, 2013, **78**, 5254–5263; (*g*) X. Z. Yu, S. J. Yu, J. Xiao, B. S. Wan and X. W. Li, *J. Org. Chem.*, 2013, **78**, 5444–5452; (*h*) W. C. Zhen, F. Wang, M. Zhao, Z. Y. Du and X. W. Li, *Angew. Chem., Int. Ed.*, 2012, **51**, 11819–11823; (*i*) L. Y. Zheng, J. Ju, Y. H. Bin and R. M. Hua, *J. Org. Chem.*, 2012, **77**, 5794–5800.

10 D. L. Davies, O. Al-Duaij, J. Fawcett, M. Giardiello, S. T. Hilton and D. R. Russell, *Dalton Trans.*, 2003, 4132–4138.

11 L. Li, W. W. Brennessel and W. D. Jones, *Organometallics*, 2009, **28**, 3492–3500.

12 PivOD was added to accelerate the H/D exchange and was required for some substrates in order to observe a substantial exchange (see ESI† for details).

13 The same general trends are observed in MeOH, however, in some cases further reaction of the product was seen. Hence, to minimise these problems, dichloromethane was used for iridium experiments. For rhodium methanol was used since the reactions are much faster in this solvent.

14 Calculations were performed with the Gaussian 03 and 09 suite of programs. The energies from gas-phase optimisations obtained with the BP86 functional were recomputed with an extended basis set and corrected for the effects of solvent (PCM approach) and dispersion (Grimme's D3 parameter set). See ESI.†

15 S. Grimme, J. Antony, S. Ehrlich and H. Krieg, *J. Chem. Phys.*, 2010, **132**, 154104.

16 This choice was also based on further functional testing that showed only BP86-D3 gave exergonic product formation for all substrates. See Table S6, ESI.†

17 The barrier for reprotonation of $\mathbf{VII_{Rh\text{-}1}}$ in MeOH is 9.3 kcal mol^{-1} while for $\mathbf{VII_{Ir\text{-}1}}$ it is 16.1 kcal mol^{-1}. The barriers to reprotonation for iridium with the other ligands are all in excess of 22 kcal mol^{-1} in MeOH, consistent with no deuterium incorporation in the exchange experiments.

18 A. G. Algarra, W. B. Cross, D. L. Davies, Q. Khamker, S. A. Macgregor, C. L. McMullin and K. Singh, *J. Org. Chem.*, 2014, 1954–1970.

19 (*a*) M. S. G. Ahlquist and P. O. Norrby, *Angew. Chem., Int. Ed.*, 2011, **50**, 11794–11797; (*b*) Y. Minenkov, G. Occhipinti and V. R. Jensen, *J. Phys. Chem. A*, 2009, **113**, 11833–11844; (*c*) U. Ryde, R. A. Mata and S. Grimme, *Dalton Trans.*, 2011, 11176–11183; (*d*) N. Sieffert and M. Bühl, *Inorg. Chem.*, 2009, **48**, 4622–4624; (*e*) Y. Zhao and D. G. Truhlar, *Org. Lett.*, 2007, **9**, 1967–1970.

